# The Impacts of Small Ice Crystals on Bulk Scattering Properties of Cirrus: Sensitivity Tests Using a New Small Ice Crystal Model and TWP-ICE Observations

**Junshik Um and Greg M. McFarquhar**
**University of Illinois, junum@atmos.uiuc.edu**

## 1. INTRODUCTION

There are considerable uncertainties on the shapes of small ice crystals (maximum dimension D < 100 μm).

Past studies assumed small ice crystals were quasi-spherical and represented them by Gaussian random spheres or droxtals.

However, a small ice analogue composed of crystalline particles (Fig. 1) grown from solution on glass substrates looks like a quasi-sphere when observed by a Cloud Particle Imager (CPI)

Because the CPI cannot distinguish between different small crystal shapes, sensitivity tests are conducted here to determine how different plausible small crystal shapes affect the calculation of bulk scattering properties.

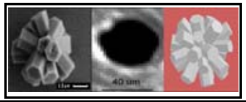

Fig.1. Ice analogue grown from solution (Ulanowski et al. 2003) (left) , imaged by CPI (middle), & newly developed small crystal model (right)

## 2. METHODOLOGY

Single-scattering properties of a new small ice crystal model 3B (Budding Bucky Ball) are calculated at $\lambda$=0.55 μm.

Bulk single-scattering properties (i.e., asymmetry parameter g) determined using observed size/shape distributions of larger crystals & different small crystal models (i.e., droxtal, Gaussian random sphere, 3B, and sphere, Fig. 2).

Size distributions from Tropical Warm Pool International Cloud Experiment (TWP-ICE) from Cloud Droplet Probe (CDP, D < 50 μm) and from Cloud Imaging Probe (CIP, D > 100 μm) from 3 days (27 and 29 Jan., 2 Feb. 2006) & 4 temperature ranges used.

Fits to the CDP and CIP data used for 50 < D < 100 μm.

Fig.2. Small ice crystal models used: Droxtal (DX, left), Gaussian random sphere (GR, middle), and 3B (right)

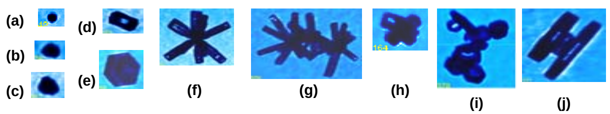


Fig.3. CPI images of shapes in classification algorithm: (a) small quasi-sphere (SQS), (b) medium quasi-sphere (MQS), (c) large quasi-sphere (LQS), (d) column (COL), (e) plate (PLT), (f) bullet rosette (BR), (g) aggregate of bullet rosettes (ABRs), (h) aggregates of columns (ACs), (i) aggregate of plate (APs), (j) capped column (CC), and unclassifiable (UC).

## 3. RESULTS

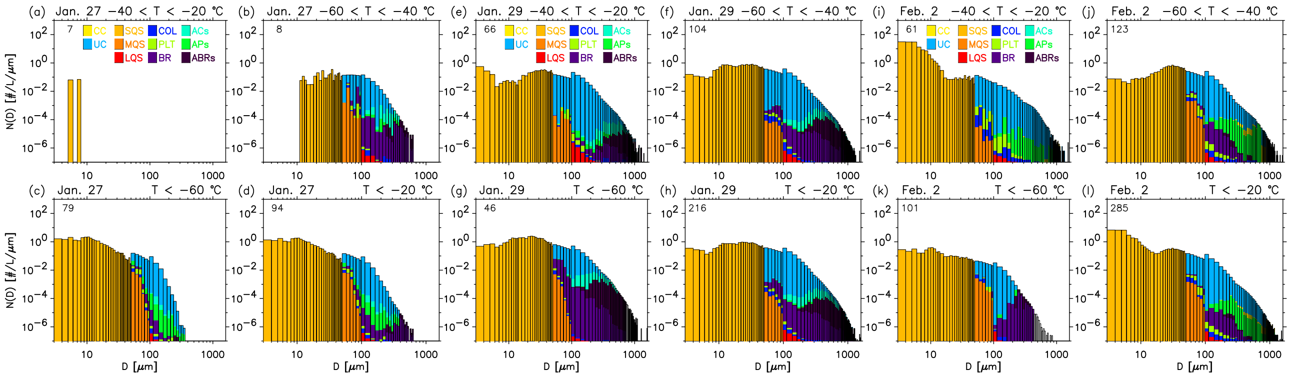


Fig.4. Average size and habit distributions as function of temperature for 27 Jan., 29 Jan., and 2 Feb. Habit distributions obtained from CPI. Four different temperature ranges considered. Total number of sampled size distributions (60 sec.) is embedded on left top of the each panel.

Using average size/habit distributions (Fig. 4) the influence of different small ice crystal models on bulk scattering properties (i.e., g) are calculated for 4 temperature ranges and 3 days (Fig. 5).

Small crystal models used are: no small crystals (NS), sphere (SP), 3B, droxtal (DX), and Gaussian random sphere (GR).

Difference (%) in g due to choice of small ice crystal model compared in Fig. 6. Influence of small crystal model greatest on 27 Jan. when more small ice crystals were present.

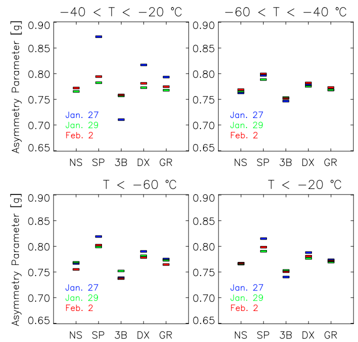


Fig.5. Calculated mean g as functions of small ice crystal model, temperature, and day

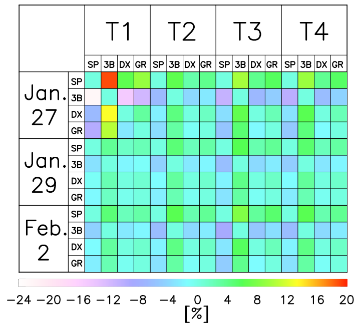


Fig.6. Difference (%) of mean g as function of small ice crystal model, temperature range and day

## 4. SUMMARY

- 29 Jan. and 2 Feb have greater fraction of large ice crystals compared to 27 Jan case (Fig. 4).
- Unclassifiable ice crystals are dominant large ice crystal habit for all 3 days (Fig. 4).
- Small ice crystals affect amount of forward scattering for all assumed models.
- Influence of small ice crystals is highest on 27 Jan. (Fig. 5 and 6).
- Using spheres for small ice crystals gives highest mean g, while using 3B gives lowest g (Fig. 5).
- Calculated mean g can vary by up to 23% depending on small ice crystal model used (Fig. 6).
- Influence of small ice crystals has minimal dependence on temperature (Fig. 5 and 6).

## ACKNOWLEDGEMENT

This research was supported by the Office of Science (BER), U.S. DOE Atmospheric Radiation Measuremt (ARM) Program Grant Numbers DE-FG02-02ER63337 and DE-FG02-07ER64378 and by the ARM Airborne Facility (AAF).